

Nagoya J. Med. Sci. 81. 41–53, 2019  
doi:10.18999/nagjms.81.1.41

## Quantitative Follow-Up Assessment of Patients with Interstitial Lung Disease by 3D-Curved High-Resolution CT Imaging Parallel to the Chest Wall

Hiroyasu Umakoshi<sup>1,2</sup>, Shingo Iwano<sup>1</sup>, Tsutomu Inoue<sup>3</sup>, Yuanzhong Li<sup>3</sup>,  
Keigo Nakamura<sup>3</sup>, and Shinji Naganawa<sup>1</sup>

<sup>1</sup>Department of Radiology, Nagoya University Graduate School of Medicine, Nagoya, Japan

<sup>2</sup>Department of Radiology, Komaki City Hospital, Komaki, Japan

<sup>3</sup>Imaging Technology Center, Fujifilm Corporation, Tokyo, Japan

### ABSTRACT

We evaluated the progression of interstitial lung disease (ILD) by three-dimensional curved high-resolution computed tomography (3D-cHRCT) at a constant depth from the chest wall and compare the results to pulmonary function test (PFT) results on a follow-up assessment. We reviewed the patients with ILD who underwent HRCT and concurrent PFTs at least twice from April 2008 to December 2014. Forty-five patients with ILD were enrolled. 3D-cHRCT images of the lung at various depths from the chest wall were reconstructed, and total area (TA), high-attenuation area (HAA) >500 HU, and %HAA ([HAA/TA] × 100) were calculated. The TA, HAA, and %HAA ratios (follow-up to baseline) were assessed for use in the diagnosis of physiologically progressive ILD (defined as; forced vital capacity [FVC] ratio <0.9 or %diffusing capacity of the lung for carbon monoxide [%DLCO] ratio <0.85 [follow-up to baseline]). Of all ratios obtained from 3D-cHRCT images at 5–30mm depths, the %HAA ratio at 20-mm had the largest area under the receiver operating characteristic curve (0.815, 95 % confidence interval 0.677–0.953). By univariate logistic regression analysis, TA, HAA, and %HAA ratios at 20-mm showed significant correlations with physiologically progressive ILD. 3D-cHRCT imaging performed in parallel with the chest wall offers novel quantitative parameters that are useful for following ILD.

Keywords: computer-aided diagnosis, quantitative imaging, interstitial lung disease, pulmonary function tests

List of Abbreviations:

3D-cHRCT: three-dimensional curved high-resolution computed tomography

CAD: computer-aided diagnosis

DLCO: diffusing capacity of the lungs for carbon monoxide

FEV1: forced expiratory volume in 1 second

FVC : forced vital capacity

HAA: high attenuation area

IP: interstitial pneumonia

ILD: interstitial lung disease

IPF: idiopathic pulmonary fibrosis

IQR: interquartile range

MDCT: multidetector computed tomography

---

Received: June 4, 2018; accepted: August 9, 2018

Corresponding Author: Shingo Iwano, MD, PhD

Department of Radiology, Nagoya University Graduate School of Medicine, 65 Tsurumai-cho, Showa-ku, Nagoya 466-8550, Japan

Tel: +81-52-744-2327, Fax; +81-52-744-2335, E-mail: iwano45@med.nagoya-u.ac.jp

OR: odds ratio  
PACS: picture archiving and communication system  
PFT: pulmonary function test  
ROC: receiver operating characteristic  
RV: residual volume  
TA: total area  
TLC: including total lung capacity  
UIP: usual interstitial pneumonia  
VC: vital capacity

This is an Open Access article distributed under the Creative Commons Attribution-NonCommercial-NoDerivatives 4.0 International License. To view the details of this license, please visit (<http://creativecommons.org/licenses/by-nc-nd/4.0/>).

## INTRODUCTION

Interstitial lung diseases (ILDs) are conditions in which inflammation and fibrosis diffusely affect the pulmonary interstitium and parenchyma, and include a variety of subsets, such as idiopathic interstitial pneumonia (IIP), collagen vascular disease related ILD and chronic hypersensitivity pneumonitis.<sup>1,2</sup> Although ILDs can show chronic or subacute progression, they sometimes show acute exacerbation leading to respiratory failure, which is associated with significant mortality.<sup>3,4</sup> Thus, patients with ILD should be monitored for progression.

Pulmonary function tests (PFTs) performed by a spirometer are often used for the diagnosis of ILD and for monitoring the disease.<sup>1</sup> Decreased total lung capacity (TLC) and vital capacity (VC) represent restrictive impairment. Diffusing capacity of the lung for carbon monoxide (DLCO) also decreases in association with the progression of ILD. Decreased values of these parameters indicate poor prognosis in patients with ILD.<sup>5</sup>

High-resolution computed tomography (HRCT) of the chest with a slice thickness  $\leq 2$  mm is a common method for the early diagnosis and follow-up of ILDs.<sup>6</sup> Moreover, HRCT has also been useful for repeated, noninvasive evaluations of patients with comorbid diseases, including emphysema, lung infections, and lung carcinoma.<sup>7</sup> The extent of fibrosis visually assessed on HRCT imaging of patients with idiopathic pulmonary fibrosis (IPF) is correlated with mortality rate, and HRCT is also useful for predicting the clinical outcomes of patients with IPF.<sup>8</sup>

To date, the use by radiologists of visual assessment of fibrosis is popular, but even experienced radiologists are subject to intra- and interobserver error.<sup>9</sup> Therefore, plans for the quantitative computer-aided diagnosis (CAD) of IP have been introduced.<sup>10-15</sup> High-speed multidetector row CT (MDCT) systems can scan the whole lung and provide sequential HRCT images, which provide increased accuracy for the evaluation of patients with emphysema and IP.

We developed a novel automated quantification system for ILD, based on the fact that most of ILD lesions extend into the peripheral lung located immediately below the chest wall, where large pulmonary vessels or bronchi, which are sometimes indistinguishable from lung abnormalities, are absent.<sup>16</sup> Our system uses serial HRCT images to automatically reconstruct a three-dimensional, curved multiplanar image of the lung at a constant depth from the chest wall. We call the method "3D curved HRCT (3D-cHRCT)". Since this novel CAD only evaluates an image depicting the zone of peripheral lung without other confusing structures, quantitative assessment of ILD is feasible.

The purpose of this study was to quantify the extent of an ILD using 3D-cHRCT at a constant depth from the chest wall, and compare the results to visual assessment and PFT results on follow-up evaluations of ILD.

## MATERIALS AND METHODS

### *Patient selection*

Our retrospective study was approved by our institutional review board, and informed consent was waived (approval No. 636–4).

We reviewed the HRCT images and the radiologists' reports, which were stored in a picture archiving and communication system (PACS), of patients with ILD opacities identified from January 2012 to December 2013. Of these 889 HRCT reports, we examined patients who had HRCT examinations and concurrent pulmonary function tests (PFTs), including diffusing capacity of the lung for carbon monoxide (DLCO) measurements at initial and follow-up evaluations (both HRCT studies were performed from January 2012 to December 2013). Of 76 patients with 110 paired study among two years, 16 paired studies with 14 patients for visually progressive ILD, and 87 paired studies for visually stable ILD were recognized. One patient with visually progressive ILD had 3 paired studies showing continuous progression, and we only took up the first paired study. To add more cases showing visual ILD progression on paired HRCT, we additionally investigated the patients who had HRCT scan from October 2012 to December 2012, and 7 paired studies were recruited with widened period of studies (April 2008 to December 2014). Totally 21 paired studies for visually progressive ILD were examined. Twenty-four paired studies for visually stable ILD were randomly recruited from the same patient lists. Their medical histories, including smoking history, past history of connective tissue disease, and the results of PFTs, were obtained from clinical records.

### *HRCT Image Acquisition and Visual Assessment*

All HRCT scans were performed using 16- or 64-MDCT scanners (Aquilion 16 and Aquilion 64; Toshiba Medical, Tokyo, Japan) in the craniocaudal direction during inspiratory apnea without contrast enhancement. The following scan parameters were used: x-ray tube voltage, 120 kVp; automatic tube-current; gantry rotation speed, 0.5 sec; and beam collimation,  $16 \times 1.0$  mm or  $64 \times 0.5$  mm. Axial thin-section CT images of whole lung were reconstructed to 1.0- or 0.5-mm slices using a high-spatial frequency algorithm (FC52 or FC86). The paired CT scan had inconsistent slice thickness in 10 case. All reconstructed CT images were transferred to the PACS at our hospital.

The axial HRCT images of extracted cases were reviewed independently by 2 chest radiologists with 4 and 21 years of experience reading thoracic CT scans. Both radiologists thereafter solved all disagreements by consensus reading of the images; and the changes over the follow-up interval, usual interstitial pneumonia (UIP) patterns, and the existence of emphysema were finally evaluated.

Fibrosis was identified on CT images as reticular opacities with peripheral and basal predominance, honeycombing, architectural distortion, and/or traction bronchiectasis or bronchiolectasis. We evaluated visual ILD progression, focusing on the CT findings as follows: (1) volume loss of the lungs, (2) increased extent of lesions (reticulation and honeycombing), (3) progression of traction bronchiectasis and architectural distortion and (4) appearance of new lesion(s) such as consolidation.<sup>17</sup> We determined the ILD progression when any 2 of the 4 findings were found on follow-up CT.

The chest radiologists visually evaluated lungs on initial axial HRCT images according the 2011 American Thoracic Society (ATS)/European Respiratory Society (ERS)/Japanese Respiratory Society (JRS)/Latin American Thoracic Association (ALAT) diagnostic criteria for UIP/IPF, and classified all cases into 3 categories, as follows: 1) definite UIP pattern (all 4 features: subpleural, basal predominance; reticular abnormality; honeycombing with or without traction bronchiectasis;

absence of features listed as inconsistent with UIP pattern), 2) possible UIP pattern (all 3 features: subpleural, basal predominance; reticular abnormality; absence of features listed as inconsistent with UIP pattern), and 3) inconsistent with UIP pattern (any of 7 features: upper or mid-lung predominance, peribronchovascular predominance, extensive ground glass abnormality [ $>$  extent of reticular abnormality], profuse micronodules [bilateral, predominantly upper lobes], discrete cysts [multiple, bilateral, away from areas of honeycombing], diffuse mosaic attenuation/air-trapping [bilateral in 3 or more lobes], consolidation in bronchopulmonary segment[s]/lobe[s]).

Emphysema was defined as well-demarcated areas of decreased attenuation as compared with contiguous normal lung, and that were margined by a very thin ( $<1$  mm) wall or no wall, and/or that showed multiple bullae ( $>1$  cm), with upper zone predominance. The severity of emphysema was evaluated visually using the Goddard classification. A score of 1 represents destruction of 1%–25% of the lung by emphysema; a score of 2, destruction of 26%–50% of the lung; a score of 3, destruction of 51%–75% of the lung; and a score of 4, destruction of 76%–100% of the lung.<sup>18</sup>

#### *Quantification of ILD by CAD*

The axial HRCT imaging data of the study patients were transferred to a 3D-workstation that automatically used our original software to reconstruct each 3D-cHRCT image of the lung 5-, 10-, 20-, and 30-mm away from the chest wall. We could not reconstruct image of 3D-cHRCT at 0-mm depth precisely, because computer could not exactly recognize the edge of lung segmentation and sometimes include chest wall itself or slight atelectasis/pleural effusion.

Figure 1 and 2 show the overall scheme of the 3D-cHRCT reconstruction procedure and examples of 3D-cHRCT images, respectively. (Fig.1) (Fig.2) Base of the lung and mediastinal pleura were not included in order to minimize the effect of normal landmark of hilar lesion and the extent of lung expansion during inspiration. The total area (TA) and high-attenuation area (HAA) (higher than the threshold value [ $>500$  HU]) of the 3D-cHRCT image were calculated by the CAD program on the workstation. The threshold value of  $>500$  HU was decided by our previous study.<sup>19</sup>

The percentage of high-attenuation area (%HAA) was defined as follows:

$$\%HAA = (HAA/TA) \times 100 (\%)$$

Moreover, to evaluate changes occurring over the interval between initial and follow-up HRCT, we determined parameter ratios as follows:

$$\begin{aligned} \text{TA ratio} &= \text{TA}_{\text{follow-up}} / \text{TA}_{\text{initial}} \\ \text{HAA ratio} &= \text{HAA}_{\text{follow-up}} / \text{HAA}_{\text{initial}} \\ \%HAA \text{ ratio} &= \%HAA_{\text{follow-up}} / \%HAA_{\text{initial}} \end{aligned}$$

Representative images of patients with stable and progressive ILD are shown with these CT values in Figure 3. (Fig.3)

#### *Pulmonary Function Tests*

PFTs were performed using a flow-sensing spirometer (FUDAC-77; Fukuda Denshi Co. Ltd., Tokyo, Japan) within 1 month of CT image acquisition. The PFT results included total lung capacity (TLC), percent predicted (%VC), forced vital capacity (FVC), forced expiratory volume in 1 second (FEV1), residual volume (RV), percent predicted (%DLCO). We determined pulmonary function parameter ratios as follows:

$$\begin{aligned} \text{TLC ratio} &= \text{TLC}_{\text{follow-up}} / \text{TLC}_{\text{initial}} \\ \%VC \text{ ratio} &= \%VC_{\text{follow-up}} / \%VC_{\text{initial}} \\ \text{FVC ratio} &= \text{FVC}_{\text{follow-up}} / \text{FVC}_{\text{initial}} \\ \text{FEV1 ratio} &= \text{FEV1}_{\text{follow-up}} / \text{FEV1}_{\text{initial}} \end{aligned}$$

## ILD follow-up evaluation by 3D-cHRCT

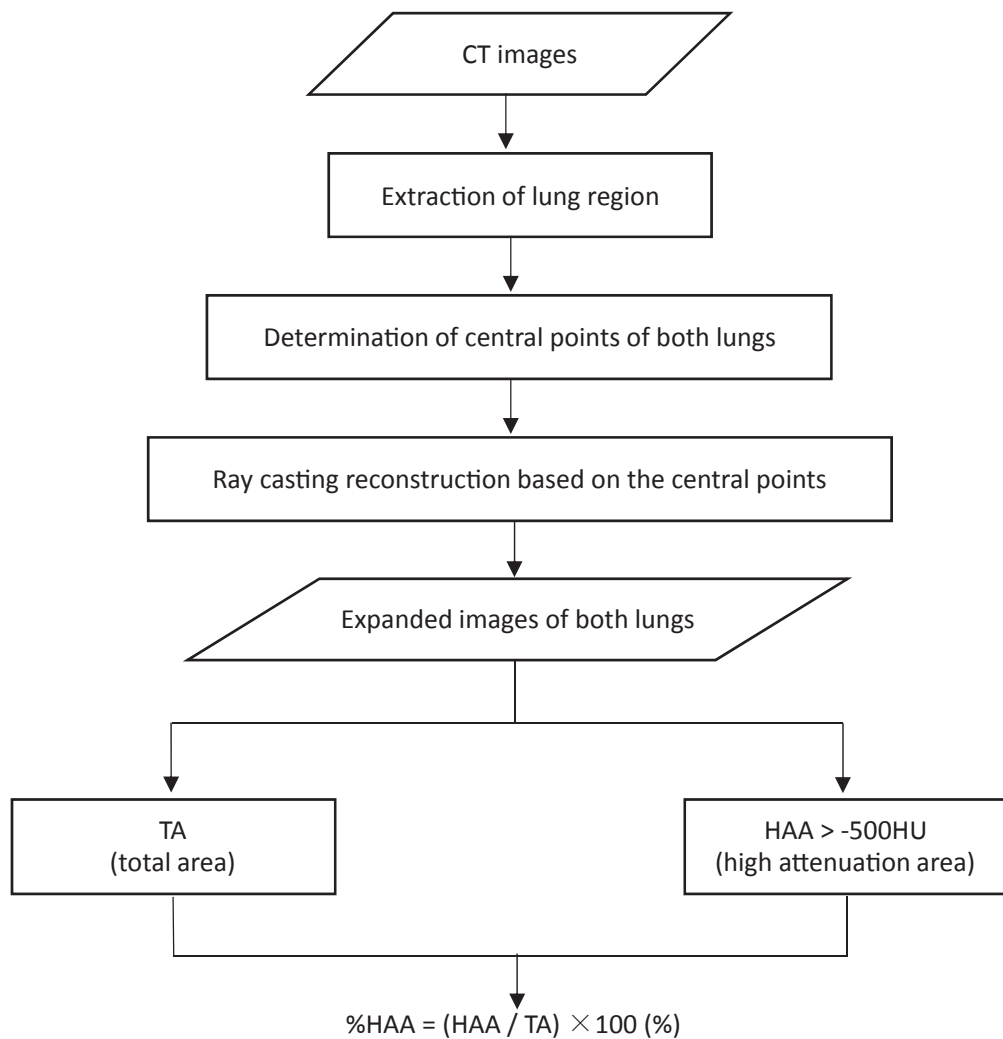


**Fig. 1 Schematic diagram of 3D-cHRCT imaging at a constant depth from the chest wall and assessment**  
 Overall schematic diagram of 3D-cHRCT image at a constant depth from the chest wall, which also shows how it is used for assessment. TA, HAA (> -500 HU), and %HAA, which were obtained from 3D-cHRCT images, were computed on a workstation using a novel CAD program.  
 3D-cHRCT three-dimensional curved high-resolution computed tomography, HAA high attenuation area, TA total area, CAD computer-aided diagnosis

$$RV \text{ ratio} = RV_{\text{follow-up}} / RV_{\text{initial}}$$

$$\%DLCO \text{ ratio} = \%DLCO_{\text{follow-up}} / \%DLCO_{\text{initial}}$$

Physiologically progressive ILD was defined as either FVC ratio <0.9 or %DLCO ratio <0.85.<sup>20</sup>

#### Statistical Analysis

First, the initial HRCT images of study patients were classified into definite/possible/inconsistent-with UIP patterns. Then, visual evidence of ILD progression and emphysema were evaluated by comparing initial with follow-up HRCT images. Kappa statistics were performed

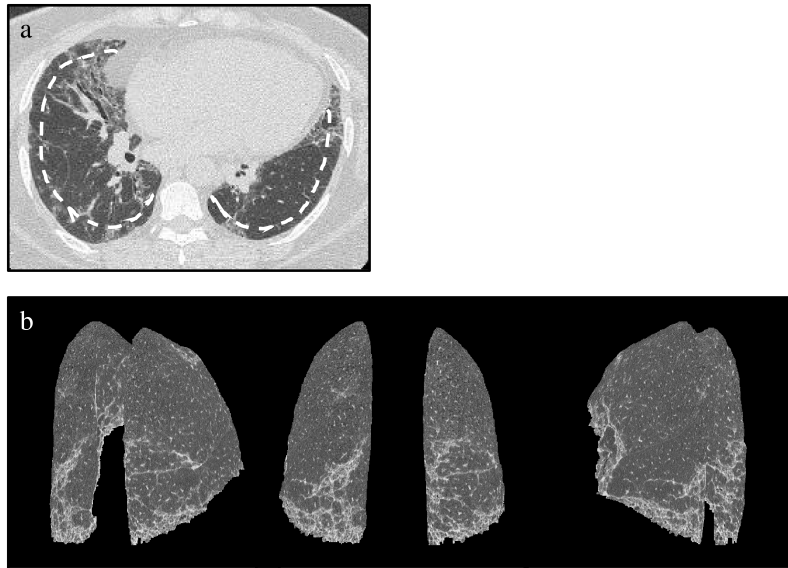


**Fig. 2 Patient with representative interstitial lung disease**

(a) Axial HRCT image and dashed line indicating 10-mm depth from the chest wall; (b) multiple-view (posterior view and posterolateral views) 3D-cHRCT images showing the 3D distribution of ILD infiltrates. 3D-cHRCT, three-dimensional curved high-resolution computed tomography; ILD interstitial lung disease

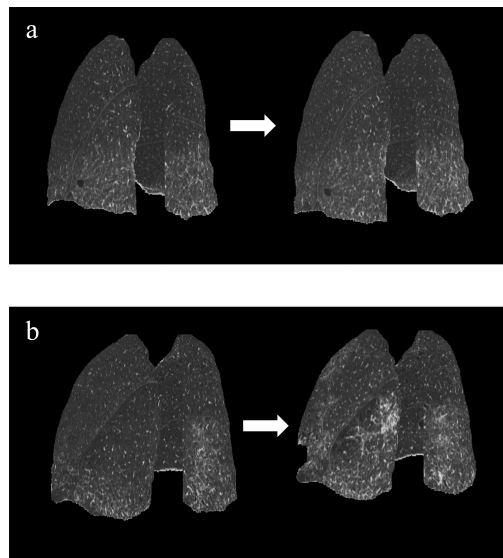


**Fig. 3 Initial and follow-up 3D-cHRCT images of representative stable and progressive ILD based on visual evaluation**

Posterolateral views of initial and follow-up 3D-cHRCT in (a) visually stable ILD and (b) visually progressive ILD. (a) Follow-up duration was 358 days. TA ratio of follow-up to initial = 1.01; HAA ratio = 1.08; %HAA ratio = 1.07. (b) Follow-up duration was 166 days. TA ratio of follow-up to initial = 0.869; HAA ratio = 1.48; %HAA ratio = 1.70.

3D-cHRCT, three-dimensional curved high-resolution computed tomography; HAA, high attenuation area; ILD, interstitial lung disease; TA, total area

to assess inter-reader agreement for the visual assessments of ILD and emphysema. Intra-reader agreement also evaluated for the visual assessment of ILD depicted on CT images. Kappa values < 0.20 were interpreted as poor, 0.21–0.40 as fair, 0.41–0.60 as moderate, 0.61–0.80 as good, and 0.81–1.00 as excellent agreement. Second, receiver operating characteristic (ROC) analyses were used to evaluate the diagnostic values of parameters quantified at 5-, 10-, 20-, and 30-mm from the chest wall in relation to the physiological progression of ILD, and optimized the quantification parameters. Third, CT parameter ratios of patients subdivided into groups based on the visual identification of ILD progression or stable disease were compared using the Student *t* test. Forth, clinical factors, CT parameter ratios, and PFT values were compared between patients with physiologically progressive ILD and stable ILD by the Student *t* test or chi-square test/ Fisher exact test. Last, correlations between individual CT parameters and physiological progression of ILD were determined using univariate logistic regression. Excel 2013 software (Microsoft Corp., Redmond, WA) and SPSS version 23.0 (IBM Corp., Armonk, NY) were used for statistical analysis.  $P < .05$  was considered statistically significant.

## RESULTS

The study included a total of 45 patients (32 men, 13 women; age range, 46–85 years; mean age, 66.7 years). The median duration until follow-up HRCT was 210 days, ranging from 31 to 1771 days. The HRCT findings were visually classified as follows: definite UIP pattern ( $n = 10$ ), possible UIP pattern ( $n = 28$ ), and inconsistent with UIP pattern ( $n = 7$ ). The kappa values for the visual assessments by the 2 radiologists were as follows: 0.753 (good agreement) for ILD progression; 0.554 (moderate) for UIP pattern; and 0.776 (good) for emphysema. Intra-reader agreement for the visual assessment of ILD depicted on HRCT images were 0.911 (excellent agreement, both 2 readers).

Seventeen patients (38%) had comorbid emphysema. Of all cases with comorbid emphysema, there was no significant change of extent of emphysema during follow-up interval. Four patients (one patient with visually progressive ILD, and three patients with visually stable ILD) suffered from lung cancer during observation periods. In the patient with progressive ILD, the size of lung cancer was increased and ILD infiltrates were also progressed. In the other patients with stable ILD, lung tumors did not show apparent enlargement.

Table 1 shows the values of the area under the ROC curve (AUC values) for each 3D-cHRCT parameter ratio in relation to the diagnosis of physiologically progressive ILD. (Table 1) The AUC of the %HAA ratio at the 20-mm distance was the highest of the all 3D-cHRCT parameters (0.815; 95 % confidence interval, 0.677–0.953). The estimated %HAA ratio cut-off value for determining progressive ILD was 1.17, with a sensitivity and specificity of 82% and 75%, respectively. Therefore, we used CT quantitative parameters obtained from 3D-cHRCT of 20-mm depth from chest wall for subsequent analyses.

Figure 4 shows the mean TA, HAA, and %HAA ratios of the patients classified with stable ILD vs progressive ILD, based on visual evaluations of HRCT images. (Fig.4) Visual progression of ILD findings was seen on the follow-up axial HRCT images of 21 patients. The mean TA ratio of patients with progressive ILD was significantly lower than the mean ratio of patients with stable ILD, and the mean HAA and %HAA ratios ( $1.50 \pm 0.56$  vs  $1.03 \pm 0.20$ ,  $P = .001$ ) of patients with progressive ILD were significantly higher than the ratios of patients with stable ILD.

Table 2 shows data for patients classified with physiologically stable ILD vs progressive ILD. (Table 2) Twenty-eight patients had physiologically stable ILD, and seventeen patients had physiologically progressive ILD. The HAA ratios ( $1.07 \pm 0.27$  vs  $1.36 \pm 0.49$ ,  $P = .014$ ) and



**Table 1** AUCs of Quantitative 3D-cHRCT Values in Relation to the Physiological Diagnosis of ILD Progression

	TA Ratio†		HAA Ratio		%HAA Ratio	
	AUC (95% CI)	P-value	AUC (95% CI)	P-value	AUC (95% CI)	P-value
<b>5 mm*</b>	0.733 (0.582 – 0.884)	.003	0.679 (0.506 – 0.851)	.042	0.700 (0.538 – 0.861)	.015
<b>10 mm</b>	0.769 (0.628 – 0.910)	<.001	0.710 (0.554 – 0.867)	.009	0.744 (0.593 – 0.894)	.002
<b>20 mm</b>	0.769 (0.630 – 0.908)	<.001	0.700 (0.525 – 0.874)	.025	0.815 (0.677 – 0.953)	<.001
<b>30 mm</b>	0.733 (0.588 – 0.878)	.002	0.754 (0.604 – 0.905)	<.001	0.777 (0.630 – 0.924)	<.001

3D-cHRCT, three-dimensional curved high-resolution computed tomography; AUC, Area under the receiver operating characteristic curve; CI, confidence interval; HAA, high attenuation area; ILD, interstitial lung disease; TA, total area

\*the distance of 3D-cHRCT images from the chest wall

†Ratio of the follow-up to baseline

**Fig. 4** 3D-cHRCT ratios at 20-mm based on visual assessment of ILD

\*Significant difference at  $P < 0.01$ , \*\* at  $P < 0.001$ .

3D-cHRCT, three-dimensional curved high-resolution computed tomography; HAA, high attenuation area; ILD, interstitial lung disease; TA, total area

%HAA ratios ( $1.09 \pm 0.37$  vs  $1.51 \pm 0.50$ ,  $P = .002$ ) at the 20-mm depth were significantly higher in patients with physiologically progressive ILD than in patients with stable ILD. The differences between the mean TA ratios of the patients with physiologically stable vs physiologically progressive ILD were also significant. The differences between the distributions of patient



**Table 2 Clinical Features and Quantitative 3D-cHRCT Data of 2 Groups of Patients with Physiologically Stable and Progressive ILD**

Physiological ILD Evaluation	Stable (n=28)	Progressive (n=17)	P-value
<b>Patient characteristics</b>			
Age (years)	66.0 ± 8.7	67.9 ± 6.9	.446
Male / Female (n)	21 / 7	11 / 6	.460
Smoking history (n)	22 (79%)	13 (76%)	.870
Connective tissue disease (n)	12 (43%)	5 (29%)	.367
CT follow up interval (day) [median, IQR]	179 [107 – 354]	358 [196 – 632]	.065
<b>Quantitative 3D-cHRCT Data</b>			
TA Ratio	0.99 ± 0.07	0.93 ± 0.08	.007
HAA Ratio	1.07 ± 0.27	1.36 ± 0.49	.014
%HAA Ratio	1.09 ± 0.37	1.51 ± 0.50	.002

3D-cHRCT, three-dimensional curved high-resolution computed tomography; HAA, high attenuation area; ILD, interstitial lung disease; IQR, interquartile range; PFT, pulmonary function test; TA, total area; UIP, usual interstitial pneumonia

**Table 3 Univariate Logistic Regression Analysis of Patient Characteristics, Quantitative 3D-cHRCT Parameters, and Visual Assessments for the diagnosis of Physiologically Progressive ILD**

Factors	OR	95% CI	P-value
<b>Patient characteristics</b>			
Age	1.03	0.95 – 1.12	.438
Male	1.64	0.44 – 6.08	.462
Smoking history	0.89	0.21 – 3.74	.870
Connective Tissue Disease	0.56	0.15 – 2.01	.370
<b>Quantitative 3D-cHRCT Values</b>			
TA Ratio (of the follow-up to baseline)	<0.0001	0 – 0.11	.016
HAA Ratio	9.76	1.21 – 78.9	.033
%HAA Ratio	13.6	1.65 – 112	.015
<b>Visual Assessment</b>			
Visually progressive	8.13	2.03 – 32.6	.003
Definite UIP pattern	1.03	0.39 – 2.77	.947
Emphysema	0.95	0.33 – 2.71	.925

3D-cHRCT, three-dimensional curved high-resolution computed tomography; CI, confidence interval; HAA, high attenuation area; OR, odds ratio; PFT, pulmonary function test; TA, total area; UIP, usual interstitial pneumonia

demographic characteristics, medical histories, according to stable and progressive disease were not significant.

Table 3 shows the results of univariate logistic regression analysis of patient clinical factors and quantitative 3D-cHRCT data in relation to physiological progression. (Table 3) The %HAA ratios at 20-mm from the chest wall were significantly correlated with the diagnosis of physiologically progressive ILD, with OR of 13.6 ( $P = .015$ ). The TA ratios and HAA ratios at 20-mm distances were also significant.

## DISCUSSION

In this study, we investigated the utility of parameters calculated at a constant depth from the chest wall for monitoring the progression of ILD. The parameters were quantified from 3D-cHRCT images reconstructed from HRCT data by our novel software. We calculated values for 3 parameters (TA, HAA, and %HAA), and we used the ratio of follow-up to initial value in order to evaluate changes in these parameters. Our results demonstrated the following 3 points: 1) Based on the ROC analysis, the %HAA ratio at the 20-mm distance from the chest wall was somewhat better diagnostic indicator for physiologically progressive ILD among 3D-cHRCT parameters investigated in this study, although there were no significant differences. 2) Differences in the mean ratios of all parameters for visually stable vs visually progressive disease were significant; 3) univariate logistic regression analysis found that TA, HAA, and %HAA ratios for 20-mm distances from the chest wall were predictive factors for physiological progression. Therefore, we conclude that this CAD system is applicable to the follow up of patients with ILD.

Various assessments are used for the diagnosis and determination of the extent of diffuse ILD, including HRCT, serology (lactate dehydrogenase, Krebs von den Lungeng-6 [KL-6], pulmonary surfactant proteins A and D), PFTs, and the 6-minute walk test.<sup>1,3</sup> However, international IPF guidelines emphasize the importance of HRCT for direct and repeated evaluations of fibrosis in the total lung. Moreover, a previous study showed that the extent of fibrosis seen on HRCT is strongly correlated with mortality rate.<sup>8</sup> Therefore, HRCT is widely considered to be essential for monitoring patients with ILDs.

Radiologists commonly perform the visual assessment of fibrosis, although even experienced radiologists are subject to intra- and interobserver error caused by misinterpretation of HRCT patterns.<sup>9</sup> In addition, reviewing and comparing serial CT findings for subtle changes, especially in patients with chronic, slowly progressive ILD, can be labor intensive. In this study, the inter-reader agreement for ILD progression was good, but not excellent. Each of radiologists had their own threshold or criteria to decide whether the subtle changes on HRCT images were significant or not. Breathing artifacts were misleading in some paired HRCT examinations. A quantitative CAD system that can easily and accurately assess changes in the imaging pulmonary manifestations of ILDs is desirable.

To date, several digital ILD quantitation systems have been developed.<sup>10-13,21,22</sup> Many of them evaluate the entire lung field and quantify each pattern of abnormality (such as consolidation, honeycombing, ground-glass opacities). However, these methods sometimes cannot differentiate an HAA reflecting lung fibrosis from normal underlying anatomic landmarks such as large blood vessels and bronchi. Manual contouring is sometimes needed, especially for bilateral hilar lesions, where there are large bronchi and vessels.<sup>23</sup> By targeting the peripheral field only, our novel quantitation system eliminates the effects of large vessels present at bilateral hilar lesions and emphasizes the peripheral predominance of fibrosis. Taking into consideration the correlation between quantitative 3D-cHRCT parameters and visually assessed progression of ILD, our novel

CAD system might be useful for assessing the extent of ILD abnormalities.

We defined physiological ILD progression as either FVC ratio  $< 0.9$  or %DLCO ratio  $< 0.85$ . The FVC and %DLCO baseline values are prognostically useful for patients with diffuse parenchymal lung diseases.<sup>5</sup> Moreover, changes in FVC and DLCO greater than 10% and greater than 15%, respectively, are generally considered to be clinically significant.<sup>24</sup> Thus, we introduced these criteria to identify clinically significant pulmonary function impairment.

Among the quantitative 3D-cHRCT parameters at 5-, 10-, 20-, and 30-mm from the chest wall, the %HAA ratio at 20-mm seemed to be a better diagnostic marker for clinically progressive ILD. Typically, lung fibrosis initially shows peripheral and basal predominance, and then with progression of disease, extends deeply into the lung. According to the histopathological classifications, the fibrosis and structural changes associated with UIP appear more frequently in the peripheral lung than abnormalities associated with other ILDs. In this study, only 10 patients were identified with a definite UIP pattern on HRCT, and we could not obtain the histopathological diagnoses of every patient. This might account for the finding that the %HAA ratio at the 20-mm distance from the chest wall was a better diagnostic marker than the %HAA ratio at the 5-, or 10-mm distance. Additionally, we have to consider that the shallow dorsal lung region is generally subject to the effects of gravity and the extent of lung expansion during inspiration. The %HAA measured at a level deeper than 30-mm from the chest wall would not easily be able to evaluate patients with mild lung fibrosis.

We hypothesized that the TA ratio would reflect changes in lung capacity associated with scarring and structural alterations, and the HAA ratio would reflect increased fibrosis or ground glass opacities. Both of these parameters were significantly correlated with visual ILD progression. However, we found that the %HAA ratio, which is derived from TA and HAA, was a better diagnostic parameter for physiologically progressive ILD.

There are several limitations to this study. First, it was a retrospective and single-center study with a small number of patients. Selection bias cannot entirely be dismissed, although the paired studies were randomly selected. Second, the diagnosis of ILD was based on radiological findings, and histopathological diagnosis was not performed for every study patient. Thus, HRCT changes in a variety of interstitial patterns based on histopathological classification were not considered. Actually, the relatively small number of patients with UIP pattern that were included in the study might affect the results. However, 3D-cHRCT might be applicable to various diffuse lung diseases. Third, the duration of follow-up intervals varied considerably, ranging from 31 to 1771 days. Patients with stable ILD often undergo annual follow-up exams, and we obtained initial and follow-up HRCT and PFT results with 1-year intervals. However, patients with progressive ILD undergo follow-up examinations when needed or available. Thus, their follow-up intervals varied widely. Fourth, we created a new threshold of HAA to evaluate the presence of fibrosis-like change in the lung, because there is no validated threshold. In this study, we adopted -500 HU as the threshold value of %HAA. However, Lederer et al used the threshold of -600 to -250HU to quantify the parenchymal lung disease on CT images,<sup>25</sup> and Sverzellati et al used 3 thresholds to quantify fibrosis-like changes (-700 to 200HU, -700 to 400HU, and -500 to 200HU) and reported that the range of density -700 to 200HU had the strongest correlation with lung function in their UIP group.<sup>26</sup> We adopted -500HU according to our previous study,<sup>19</sup> but this threshold would be affected by the CT scanner, reconstruction kernel, etc. We need further study to improve the threshold of HAA more appropriate. Fifth, we did not consider the influence of factors other than ILD progression for the PFTs and DLCO, such as increase of emphysema. In this study, there was no significant change of the extent of emphysema, and we expect less influence by the existence of emphysema.

## CONCLUSIONS

In conclusion, 3D-CHRCT imaging performed in parallel with the chest wall offers novel quantitative parameters that are significantly correlated both with visual and physiological progression of ILDs on a follow-up assessment.

## ACKNOWLEDGMENTS

This study has received funding by Japan Society for the Promotion of Science (JSPS) Grant-in-Aid for Scientific Research on Innovative Areas (Multidisciplinary Computational Anatomy), JSPS KAKENHI Grant Number 17H05292.

We would like to thank JAM Post for their helpful advice in writing the English manuscript.

## CONFLICT OF INTEREST

TI, YL and KN are employees of Fujifilm corporation. However, Fujifilm corporation had no control over the interpretation, writing, or publication of this work.

## REFERENCES

- 1 American Thoracic Society/European Respiratory Society International Multidisciplinary Consensus Classification of the Idiopathic Interstitial Pneumonias. This joint statement of the American Thoracic Society (ATS), and the European Respiratory Society (ERS) was adopted by the ATS board of directors, June 2001 and by the ERS Executive Committee, June 2001. *Am J Respir Crit Care Med.* 2002;165(2):277–304.
- 2 Travis WD, Costabel U, Hansell DM, et al. An official American Thoracic Society/European Respiratory Society statement: update of the international multidisciplinary classification of the idiopathic interstitial pneumonias. *Am J Respir Crit Care Med.* 2013;188(6):733–748.
- 3 Wallis A, Spinks K. The diagnosis and management of interstitial lung diseases. *BMJ (Clinical research ed).* 2015;350:h2072.
- 4 Taniguchi H, Kondoh Y. Acute and subacute idiopathic interstitial pneumonias. *Respirology.* 2016;21(5):810–820.
- 5 Martinez FJ, Flaherty K. Pulmonary function testing in idiopathic interstitial pneumonias. *Proc Am Thorac Soc.* 2006;3(4):315–321.
- 6 Raghu G, Collard HR, Egan JJ, et al. An official ATS/ERS/JRS/ALAT statement: idiopathic pulmonary fibrosis: evidence-based guidelines for diagnosis and management. *Am J Respir Crit Care Med.* 2011;183(6):788–824.
- 7 Raghu G, Amatto VC, Behr J, Stowasser S. Comorbidities in idiopathic pulmonary fibrosis patients: a systematic literature review. *Eur Respir J.* 2015;46(4):1113–1130.
- 8 Gay SE, Kazerooni EA, Toews GB, et al. Idiopathic pulmonary fibrosis: predicting response to therapy and survival. *Am J Respir Crit Care Med.* 1998;157(4 Pt 1):1063–1072.
- 9 Watadani T, Sakai F, Johkoh T, et al. Interobserver variability in the CT assessment of honeycombing in the lungs. *Radiology.* 2013;266(3):936–944.
- 10 Yoon RG, Seo JB, Kim N, et al. Quantitative assessment of change in regional disease patterns on serial HRCT of fibrotic interstitial pneumonia with texture-based automated quantification system. *Eur Radiol.* 2013;23(3):692–701.
- 11 Shin KE, Chung MJ, Jung MP, Choe BK, Lee KS. Quantitative computed tomographic indexes in diffuse interstitial lung disease: correlation with physiologic tests and computed tomography visual scores. *J Comput Assist Tomogr.* 2011;35(2):266–271.
- 12 Iwasawa T, Asakura A, Sakai F, et al. Assessment of prognosis of patients with idiopathic pulmonary fibrosis by computer-aided analysis of CT images. *J Thorac Imaging.* 2009;24(3):216–222.
- 13 Bartholmai BJ, Raghunath S, Karwoski RA, et al. Quantitative computed tomography imaging of interstitial

- lung diseases. *J Thorac Imaging*. 2013;28(5):298–307.
- 14 Kim HG, Tashkin DP, Clements PJ, et al. A computer-aided diagnosis system for quantitative scoring of extent of lung fibrosis in scleroderma patients. *Clin Exp Rheumatol*. 2010;28(5 Suppl 62):S26–35.
  - 15 Uppaluri R, Hoffman EA, Sonka M, Hartley PG, Hunninghake GW, McLennan G. Computer recognition of regional lung disease patterns. *Am J Respir Crit Care Med*. 1999;160(2):648–654.
  - 16 Sverzellati N, Lynch DA, Hansell DM, Johkoh T, King TE, Jr., Travis WD. American Thoracic Society-European Respiratory Society Classification of the idiopathic interstitial pneumonias: advances in knowledge since 2002. *Radiographics*. 2015;35(7):1849–1871.
  - 17 Iwasawa T, Ogura T, Sakai F, et al. CT analysis of the effect of pirfenidone in patients with idiopathic pulmonary fibrosis. *Eur J Radiol*. 2014;83(1):32–38.
  - 18 Goddard PR, Nicholson EM, Laszlo G, Watt I. Computed tomography in pulmonary emphysema. *Clin Radiol*. 1982;33(4):379–387.
  - 19 Umakoshi H, Iwano S, Inoue T, Li Y, Naganawa S. Quantitative evaluation of interstitial pneumonia using 3D-curved high-resolution CT imaging parallel to the chest wall: a pilot study. *PLoS One*. 2017;12(9):e0185532.
  - 20 Kondoh Y, Taniguchi H, Ogura T, et al. Disease progression in idiopathic pulmonary fibrosis without pulmonary function impairment. *Respirology*. 2013;18(5):820–826.
  - 21 Koyama H, Ohno Y, Yamazaki Y, et al. Quantitatively assessed CT imaging measures of pulmonary interstitial pneumonia: effects of reconstruction algorithms on histogram parameters. *Eur J Radiol*. 2010;74(1):142–146.
  - 22 Matsuoka S, Yamashiro T, Matsushita S, et al. Morphological disease progression of combined pulmonary fibrosis and emphysema: comparison with emphysema alone and pulmonary fibrosis alone. *J Comput Assist Tomogr*. 2015;39(2):153–159.
  - 23 Adams H, Bernard MS, McConnochie K. An appraisal of CT pulmonary density mapping in normal subjects. *Clin Radiol*. 1991;43(4):238–242.
  - 24 Ley B, Collard HR, King TE, Jr. Clinical course and prediction of survival in idiopathic pulmonary fibrosis. *Am J Respir Crit Care Med*. 2011;183(4):431–440.
  - 25 Lederer DJ, Enright PL, Kawut SM, et al. Cigarette smoking is associated with subclinical parenchymal lung disease: the Multi-Ethnic Study of Atherosclerosis (MESA)-lung study. *Am J Respir Crit Care Med*. 2009;180(5):407–414.
  - 26 Sverzellati N, Calabro E, Chetta A, et al. Visual score and quantitative CT indices in pulmonary fibrosis: Relationship with physiologic impairment. *Radiol Med*. 2007;112(8):1160–1172.

